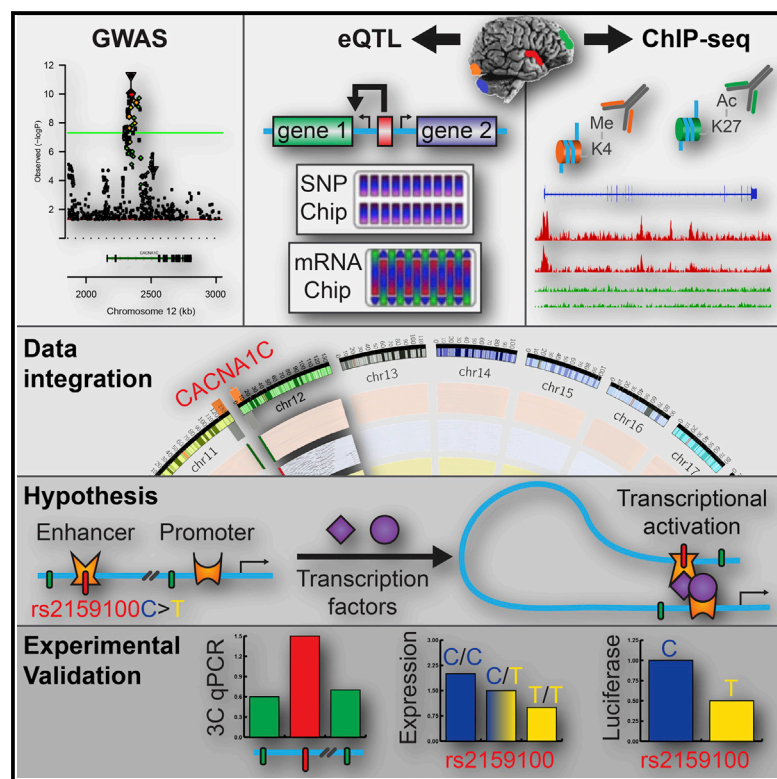


A Role for Noncoding Variation in Schizophrenia

Graphical Abstract



Highlights

Schizophrenia SNPs are enriched for eQTLs and *cis*-regulatory elements

The enrichment is greater for enhancers in fetal and adult brain tissue

Schizophrenia risk SNPs participate in long-range promoter-enhancer interactions

CACNA1C variants are associated with transcriptional regulation in the brain

Authors

Panos Roussos, Amanda C. Mitchell, ..., Schahram Akbarian, Pamela Sklar

Correspondence

panagiotis.roussos@mssm.edu (P.R.),
pamela.sklar@mssm.edu (P.S.)

In Brief

Roussos et al. find that schizophrenia risk variants are enriched for alleles that affect gene expression and lie within promoters or enhancers. For the L-type calcium channel (*CACNA1C*), the risk variant is associated with transcriptional regulation in the brain and is positioned within an enhancer sequence that physically interacts through chromosome loops with the promoter region of the gene.

Accession Numbers

GSE62391



A Role for Noncoding Variation in Schizophrenia

Panos Roussos,^{1,2,3,4,5,20,*} Amanda C. Mitchell,^{1,4,6,20} Georgios Voloudakis,^{1,4,6} John F. Fullard,^{1,4} Venu M. Pothula,^{1,4,6} Jonathan Tsang,¹ Eli A. Stahl,^{1,2,3} Anastasios Georgakopoulos,¹ Douglas M. Ruderfer,^{1,2,3} Alexander Charney,^{1,2,3} Yukinori Okada,^{7,8} Katherine A. Siminovitch,^{9,10,11} Jane Worthington,^{12,13} Leonid Padyukov,¹⁴ Lars Klareskog,¹⁴ Peter K. Gregersen,¹⁵ Robert M. Plenge,^{16,17,18} Soumya Raychaudhuri,^{16,17,18,19} Menachem Fromer,^{1,2,3} Shaun M. Purcell,^{1,2,3} Kristen J. Brennand,^{1,4,6} Nikolaos K. Robakis,^{1,4,6} Eric E. Schadt,^{2,3} Schahram Akbarian,^{1,4,6,21} and Pamela Sklar^{1,2,3,4,6,21,*}

¹Department of Psychiatry, Icahn School of Medicine at Mount Sinai, New York, NY 10029, USA

²Department of Genetics and Genomic Sciences, Icahn School of Medicine at Mount Sinai, New York, NY 10029, USA

³Institute for Genomics and Multiscale Biology, Icahn School of Medicine at Mount Sinai, New York, NY 10029, USA

⁴Friedman Brain Institute, Icahn School of Medicine at Mount Sinai, New York, NY 10029, USA

⁵James J. Peters VA Medical Center, Mental Illness Research Education and Clinical Center (MIRECC), 130 West Kingsbridge Road, Bronx, NY 10468, USA

⁶Department of Neuroscience, Icahn School of Medicine at Mount Sinai, New York, NY 10029, USA

⁷Department of Human Genetics and Disease Diversity, Graduate School of Medical and Dental Sciences, Tokyo Medical and Dental University, Tokyo 230-0045, Japan

⁸Laboratory for Statistical Analysis, RIKEN Center for Integrative Medical Sciences, Yokohama 230-0045, Japan

⁹Lunenfeld-Tanenbaum Research Institute, Mount Sinai Hospital, Toronto, ON M5G 1X5, Canada

¹⁰Toronto General Research Institute, Toronto, ON M5G 2M9, Canada

¹¹Department of Medicine, University of Toronto, Toronto, ON M5S 2J7, Canada

¹²Arthritis Research UK Centre for Genetics and Genomics, Musculoskeletal Research Centre, Institute for Inflammation and Repair, Manchester Academic Health Science Centre, University of Manchester, Manchester M13 9NT, UK

¹³National Institute for Health Research, Manchester Musculoskeletal Biomedical Research Unit, Central Manchester University Hospitals National Health Service Foundation Trust, Manchester Academic Health Sciences Centre, Manchester M13 9NT, UK

¹⁴Rheumatology Unit, Department of Medicine (Solna), Karolinska Institutet, Stockholm 171 76, Sweden

¹⁵The Feinstein Institute for Medical Research, North Shore-Long Island Jewish Health System, Manhasset, NY 11030, USA

¹⁶Division of Rheumatology, Immunology, and Allergy, Brigham and Women's Hospital, Harvard Medical School, Boston, MA 02115, USA

¹⁷Division of Genetics, Brigham and Women's Hospital, Harvard Medical School, Boston, MA 02115, USA

¹⁸Program in Medical and Population Genetics, Broad Institute, Cambridge, MA 02142, USA

¹⁹NIHR Manchester Musculoskeletal Biomedical Research Unit, Central Manchester NHS Foundation Trust, Manchester Academic Health Sciences Centre, Manchester M13 9NT, UK

²⁰Co-first author

²¹Co-senior author

*Correspondence: panagiotis.roussos@mssm.edu (P.R.), pamela.sklar@mssm.edu (P.S.)

<http://dx.doi.org/10.1016/j.celrep.2014.10.015>

This is an open access article under the CC BY license (<http://creativecommons.org/licenses/by/3.0/>).

SUMMARY

A large portion of common variant loci associated with genetic risk for schizophrenia reside within noncoding sequence of unknown function. Here, we demonstrate promoter and enhancer enrichment in schizophrenia variants associated with expression quantitative trait loci (eQTL). The enrichment is greater when functional annotations derived from the human brain are used relative to peripheral tissues. Regulatory trait concordance analysis ranked genes within schizophrenia genome-wide significant loci for a potential functional role, based on colocalization of a risk SNP, eQTL, and regulatory element sequence. We identified potential physical interactions of noncontiguous proximal and distal regulatory elements. This was verified in prefrontal cortex and -induced pluripotent stem cell-derived neurons for the L-type calcium channel (*CACNA1C*) risk locus.

Our findings point to a functional link between schizophrenia-associated noncoding SNPs and 3D genome architecture associated with chromosomal loopings and transcriptional regulation in the brain.

INTRODUCTION

A recent multistage genome-wide association study (GWAS) in schizophrenia (SCZ) identified 22 linkage disequilibrium (LD)-independent loci that reached genome-wide significance (Ripke et al., 2013). The majority of identified SNPs reside within noncoding regions of genes or in intergenic regions. Furthermore, the regions were frequently large and often contained multiple implicated SNPs due to local LD patterns. In order to be able to understand these associations mechanistically, it is important to develop strategies for honing in on regions and SNPs more likely to have functional effects. Thus, the elucidation of the function of noncoding disease-associated loci is an important next step toward the development of testable hypotheses regarding biological processes involved in the pathogenesis of SCZ.

Table 1. SNP Enrichment for Different GWAS p Values

Functional Category	Number of SNPs		Number of SNPs (SNP Enrichment)					
			$p < 10^{-3}$		$p < 10^{-5}$		$p < 5 \times 10^{-8}$	
	CRE	creSNP	CRE	creSNP	CRE	creSNP	CRE	creSNP
SCZ GWAS	9,815,700		42,253		4,337		692	
eSNP	1,479,508		15,762 (3.68)		2,585 (8.07)		529 (14.13)	
Active promoter (H3K4me3 and [H3K9ac or H3K27ac])	209,349	51,728	1,363 (2.13)	778 (5.17)	172 (2.88)	142 (9.31)	18 (4.57)	17 (17.38)
Active enhancer (H3K4me1 and [H3K9ac or H3K27ac])	419,981	95,701	2,858 (2.30)	1,518 (5.66)	353 (3.16)	290 (11.46)	59 (7.08)	54 (29.51)
DHS	276,468	46,770	1,365 (1.58)	558 (4.06)	158 (2.39)	118 (10.94)	26 (5.13)	23 (26.92)
Poised promoter (H3K4me3 and H3K27me3)	81,260	13,743	357 (1.4)	155 (4.03)	27 (1.02)	25 (5.36)	3 (2.29)	3 (13.80)
Repressed enhancer (H3K4me1 and H3K27me3)	165,117	25,547	623 (1.13)	241 (3.12)	46 (0.82)	34 (4.67)	5 (1.51)	5 (9.55)

The enrichment of each functional category is given in comparison to FUV.

Across many phenotypes, noncoding GWAS risk loci are involved in the regulation of transcriptional activity and demonstrate enrichment for expression quantitative trait loci (Nicolae et al., 2010; Richards et al., 2012; Zhong et al., 2010) and *cis*-regulatory elements (CREs) (Degner et al., 2012; Harismendy et al., 2011; Maurano et al., 2012; Musunuru et al., 2010). A CRE, such as a promoter or an enhancer, is a noncoding DNA sequence in, near, or distal to a gene that contains binding sites for regulatory factors and is required for proper spatiotemporal expression of the gene. Long-distance enhancers are thought to interact physically with gene proximal promoters and transcription start sites (TSSs) by forming loops through regulatory proteins including cohesins and other repressors and facilitators of transcription (Fanucchi et al., 2013; Kagey et al., 2010). Because these chromosomal loopings can bypass hundreds of kilobases on the linear genome, risk loci positioned within CREs at a distance from the TSS could affect the binding of these regulatory proteins and ultimately lead to allele-specific differences in target gene expression and subsequent alterations in molecular pathways implicated in disease.

In this study, we use functional annotations to categorize GWAS SNPs and demonstrate that variants increasing risk for SCZ are enriched for alleles that affect gene expression (eSNPs) and lie within promoters or enhancers. The enrichment shows tissue specificity and is greatest when functional annotations derived from human cerebral cortex are used. For ten out of 22 SCZ GWAS hits, we identify functional variants positioned within promoters, enhancers, and other regulatory sequences that are associated with expression of 13 genes. For the L-type calcium channel (*CACNA1C*), a well-established SCZ risk locus, we map noncontiguous physical interactions between enhancer regions and the TSSs using human postmortem brain tissue and human induced pluripotent stem cells (hiPSCs)-derived neurons. Overall, this study provides a functional link between SCZ noncoding risk loci and physical interactions of noncontiguous DNA elements associated with transcriptional regulation in the human brain.

RESULTS

Enrichment of Functional Annotation Categories in SCZ

We primarily used publically available data to generate functional annotations. Brain eSNPs were generated by using genotype and gene-expression profiles from eight data sets (Colantuoni et al., 2011; Gibbs et al., 2010; Zhang et al., 2014; Table S1). The brain CRE annotation map was generated based on chromatin immunoprecipitation followed by high-throughput sequencing (ChIP-seq) experiments of histone modifications (Cheung et al., 2010; Maurano et al., 2012; Shulha et al., 2012, 2013; Zhu et al., 2013; Tables S2 and S3). We integrated data from specific sets of histone methylation and acetylation markings and DNase I hypersensitive sites (DHSs) to define five types of CREs: active promoter; active enhancer; poised promoter; repressed enhancer; and open chromatin regions.

Genome-wide SNPs from a published SCZ GWAS data set (Ripke et al., 2013) were classified into four different categories: (1) eSNP: if they affect gene expression of specific transcripts; (2) CRE: if they lie within a CRE region; (3) eSNP in a *cis*-regulatory element (creSNP); or (4) functionally unannotated variants (FUV), if they did not cluster to any of the above categories (Table S4). Among SCZ nominally associated loci at $p \leq 10^{-3}$ ($n = 42,253$ SNPs), 37.3% were grouped into the eSNP category ($n = 15,762$; Table 1). Among this 37.3%, 4.9% were in active promoters, 9.6% in active enhancers, 3.5% in DHSs, 1.0% in poised promoters, and 1.5% in repressed enhancers. Relative enrichments for the categories were calculated using an empirical cumulative distribution of the GWAS p values after controlling for genomic inflation as described previously (Schork et al., 2013). Across all p value thresholds tested, the largest enrichment of GWAS SNPs occurs in the following categories: eSNPs and three types of CREs: active promoters, active enhancers, and DHSs (Table 1; Figure 1). Despite having fewer SNPs, enrichment is greater when the combined creSNP functional category is analyzed for all types of CREs (CRE range: 1.58- to 7.08-fold; creSNP range: 4.03- to 29.51-fold). This indicates that SCZ-associated variants are enriched for SNPs that have stronger support for a functional role (creSNP). Higher

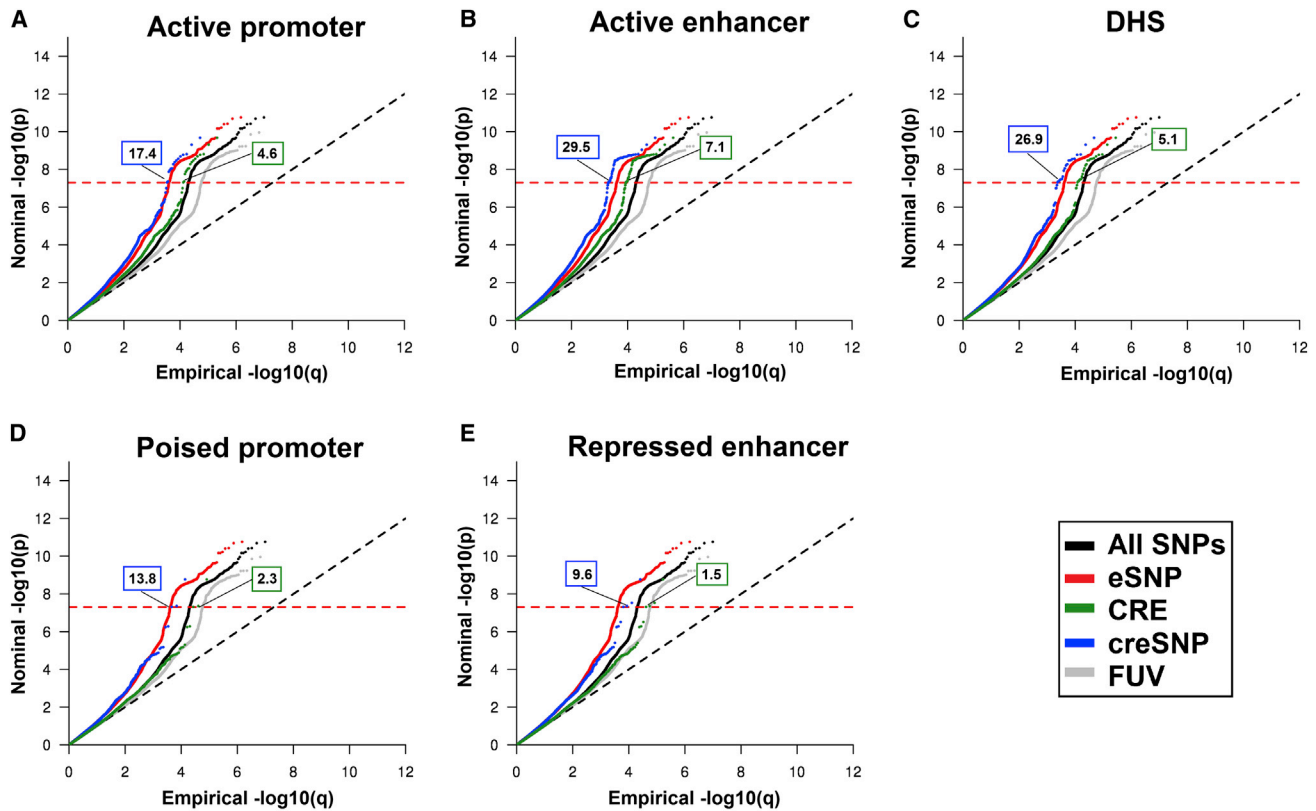


Figure 1. Stratified Q-Q Plots for eSNP, CRE, and creSNP in Active Promoter, Active Enhancer, DHS, Poised Promoter, and Repressed Enhancer Functional Annotation Categories

The numbers for each functional category (blue box: creSNP; green box: CRE) illustrate the estimated increase in terms of the proportion of p values expected below a genome-wide significant p value ($p < 5 \times 10^{-8}$; red dashed line) compared to the functionally unannotated variant (FUV) category. The estimated enrichment for eSNPs is 14.1. For all functional categories, enrichment is greater when the creSNP functional category is analyzed relative to CREs. All summary statistics were corrected for inflation by using the FUV inflation control. The major histocompatibility complex locus (chr6: 25–35 Mb) was excluded from the SCZ data set.

enrichment of the creSNP in comparison to CRE categories alone is found for the individual, nonintegrated CRE and creSNP functional annotation categories (Figure S1; Table S5). Among the individual, nonintegrated creSNP annotations, H3K4me1, an individual histone mark of enhancers, in fetal and adult brain tissue is the most-enriched category (Table S5).

We provide a single number quantification of enrichment by calculating a categorical enrichment score (CES), which is a conservative estimate of the variance attributable to nonnull SNPs (Schork et al., 2013). The CES analysis indicates the following: first, SNPs that cluster within CRE, eSNP, and creSNP functional annotation categories show higher CES compared to FUV (Figure 2). Second, the creSNP categories (scaled CES creSNP range: 0.66–1) have higher CES than CREs (scaled CES CRE range: 0.11–0.29). Third, certain creSNP categories (active promoter, active enhancer, and DHS) were the most enriched as measured by the CES. The enrichment was significant for active promoter and enhancer (for both CRE and creSNP), eSNP, and DHS creSNP (all $p \leq 0.0001$ by permutation). In the individual nonintegrated functional categories, the H3K4me1 and H3K4me3 creSNP annotations in fetal brain tissue were

the most enriched (26-fold compared to FUV category; $p \leq 0.0001$ by permutation), as measured by the CES (Figure S2).

Differences in the extent of LD (estimated based on the sum r^2) and minor allele frequency (MAF) were observed between the functional categories (Table S6). Because categories with higher average MAF or larger total amount of LD could spuriously appear enriched for SCZ association, we performed regression analysis, which demonstrated that the effect of functional categories remains independently strong with an effect size rank that mirrors enrichment, despite the significant correlation among categories (Table S7). Furthermore, the enrichment was significant for all functional categories compared to FUV after removing SNPs with $r^2 > 0.1$ and those that were < 100 kb from a more strongly associated variant in the SCZ study (Table S6; Figure S3).

Tissue Specificity of Functional Annotation Categories for GWAS Enrichment

We then examined whether functional categories generated in brain tissue can better inform SCZ SNPs (show higher CES) compared to annotations derived from nonbrain tissues. We

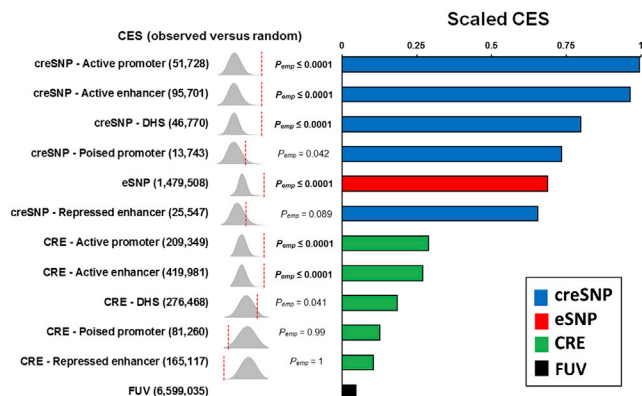


Figure 2. Categorical Enrichment for the Combined Functional Annotations as Measured by the CES

On the left side, we show the observed enrichment (red dashed lines) against the null distribution (gray density plots). For each functional category, we performed 10,000 permutations to calculate the null distribution of enrichment for comparison to observed categorical enrichment. Functional categories with empirical p values that survived Bonferroni multiple testing correction are in bold (p corrected: $0.05/11 = 4.5 \times 10^{-3}$). The number in parentheses indicates the number of SNPs per annotation category. On the right side, the bar plot illustrates the scaled CES for each functional category. creSNPs are illustrated in blue color, eSNPs in red, CREs in green, and FUV in black. The CESs are scaled using the maximum value across functional categories. All summary statistics were corrected for inflation by using the FUV inflation control.

used the following nonbrain eSNP-lymphoblastoid cell line (LCL) (Xia et al., 2012), liver (Innocenti et al., 2011), peripheral blood mononuclear cells (PBMCs) (Westra et al., 2013), skin, and adipose tissue (Grundberg et al., 2012)—and CRE-skin, T-helper, liver, and adipose tissue (Maurano et al., 2012; Zhu et al., 2013)—functional categories to estimate CES for SCZ GWAS as described above. In addition, we calculated CES using a previously published GWAS in rheumatoid arthritis (RA) (Stahl et al., 2010). The PBMC eSNP and T-helper CRE functional categories were selected as positive controls for RA because immunological cells are implicated in its etiopathogenesis (Okada et al., 2014; Trynka et al., 2013). The major histocompatibility complex (MHC) locus (chr6: 25–35 Mb) was excluded from both GWAS data sets. The brain eSNP and CRE functional category showed the highest enrichment for SCZ (Figure 3A). In contrast, the blood/T-helper functional category showed the highest enrichment for RA. Within the brain and blood/T-helper related functional categories, the active promoter, active enhancer, and DHS show the highest enrichment for SCZ and RA SNPs, respectively (Figure 3B).

Using Functional Annotations to Prioritize Risk Loci in SCZ

The majority of SCZ genome-wide significant loci (index and SNPs in LD with them) are noncoding (Ripke et al., 2013). Given the enrichment of SCZ loci for eSNPs, we used the regulatory trait concordance (RTC) approach (Grundberg et al., 2012; Nica et al., 2010) to prioritize SNPs and genes within SCZ genome-wide significant loci. RTC scores ≥ 0.9 indicate that overlapping eSNP and GWAS signals likely tag the same variant.

The genome-wide significant SNPs in Ripke et al. were mapped to 22 hot spot intervals (Table 2). We detected overlapping eSNP and GWAS signals at $RTC \geq 0.9$ for 10 of 22 intervals, four times the number expected by chance (2.2 expected in the top 10% of scoring intervals under the uniform distribution; Nica et al., 2010; $p = 2 \times 10^{-5}$). The SCZ-related eSNPs are associated with expression of 17 genes (three intervals had RTC scores with eSNPs of ≥ 0.9 for more than one gene). Given the enrichment of SCZ loci for creSNPs, we examined whether any of the 17 SCZ-associated eSNPs (and tag SNPs within 500 kb and $r^2 > 0.8$) lie within the most-enriched CRE categories (active promoter, active enhancer, and DHS). Thirteen eSNPs out of the 17 are localized within such a CRE (Table 2; Figure 4). The expression of five genes is associated with loci within enhancers (*C10orf32*, *CACNA1C*, *NGEF*, *RP11-490G2.2*, and *SDCCAG8*). Gene expression of *AS3MT* is influenced by an eSNP that lies within the promoter region. The expression level of the remaining genes (*NT5C2*, *GATAD2A*, *HAPLN4*, *GNL3*, *NEK4*, *SPCS1*, and *TYW5*) is associated with multiple eSNPs within both promoter and enhancer sequences.

Functional Annotations Identify Risk Variants in *CACNA1C* that Lie within Putative Enhancers and Affect Gene Expression

The stepwise approach described above (Table 2; Figure 4) allows us to formulate a testable hypothesis for the mechanism through which some variants might increase risk for SCZ. For example, the *CACNA1C* index SNP (rs1006737) and eSNP (rs758170) are in close proximity (16.2 kb) and have an RTC score of 1. Furthermore, the risk allele is associated with decreased *CACNA1C* gene expression ($p = 1.88 \times 10^{-5}$ at false discovery rate [FDR] 0.7%). We identified four SNPs (rs2159100, rs12315711, rs11062170, and rs4765905) that are in perfect LD with rs758170 and rs1006737 and lie within two predicted enhancers (spanning 1.4 kb and 1.85 kb), ~ 185 kb downstream from the gene's TSS (Figures 5A and 5B). To identify whether the predicted enhancer region might be capable of forming promoter-enhancer loops, we mapped its physical interaction with the *CACNA1C* TSS in human dorsolateral prefrontal cortex ($n = 6$) and hiPSC-derived neurons by chromosome conformation capture (3C) assay (Mitchell et al., 2014; Tables S8 and S9). In addition, this approach allows us to dissect the LD complexity of the region and identify variants with additional support for a functional role. Of the 17 restriction site regions tested, only one displayed an increased interaction with the TSS in human postmortem tissue (primer no. 4 in Figures 5A–5D). This enhancer region includes rs2159100 (MAF = 0.35; GWAS p value = 1.1×10^{-10}) and rs12315711 (MAF = 0.35; GWAS p value = 1.1×10^{-10}) and demonstrates increased interaction frequency with the *CACNA1C* promoter ($F[16, 83] = 5.52$; $p = 8 \times 10^{-8}$). The rs2159100/rs12315711 3C interaction was confirmed in hiPSC-derived neurons (Figure 5D). In addition to being in an enhancer region, rs2159100 also colocalizes with a 600 bp DHS region. Thus, we examined its effect on transcriptional activity in *in vitro* experiments. Compared to the reference rs2159100 C allele, the risk T variant is associated with decreased transcriptional activity in human embryonic kidney 293 (HEK293) and Neuro-2a cells

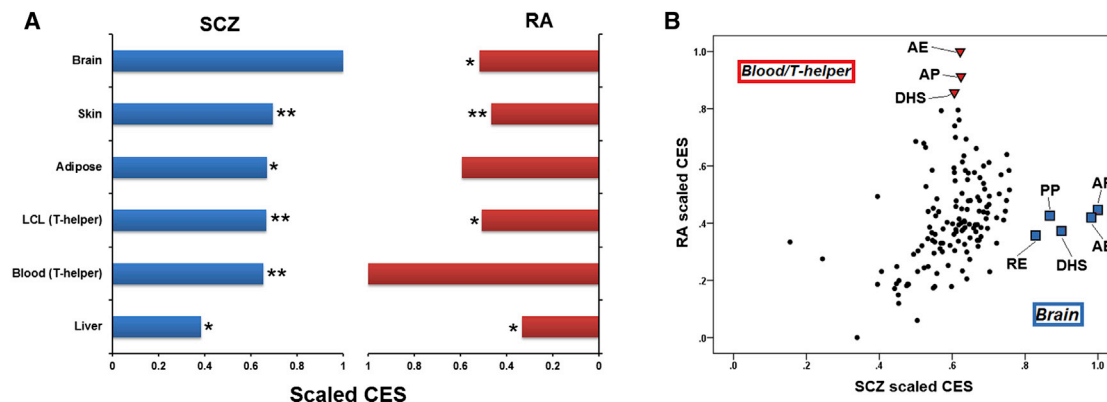


Figure 3. Categorical Enrichment in the SCZ and RA GWAS Data Sets for eSNPs and CREs

For each eSNP-CRE combination, the (A) average value of the CES across all functional categories (active promoter, active enhancer, DHS, poised promoter, and repressed enhancer) or (B) individual value was calculated. For each GWAS data set, the CESs were scaled using the maximum value across functional categories. The brain- and blood/T-helper-related eSNP and CRE functional category showed the highest enrichment for SCZ (blue) and RA (red) SNPs, respectively. All summary statistics were corrected for inflation by using the FUV inflation control. * $p < 0.05$ and ** $p < 0.01$ by nonparametric Mann-Whitney among the most-enriched category and the rest of functional categories for each GWAS data set. AE, active enhancer; AP, active promoter; PP, poised promoter; RE, repressed enhancer.

(42% [$p < 0.0001$] and 23% [$p < 0.05$] reduction in luciferase activity, respectively; Figure 5E).

DISCUSSION

We have demonstrated that SCZ-associated loci are enriched for certain functional annotation categories. As reported previously, we found enrichment with eSNPs (Richards et al., 2012) and CRE annotations, highlighting active regulatory regions (Trynka et al., 2013). Here, we demonstrate that integrative analysis of eSNPs with CRE epigenomic annotations identifies greater enrichment of risk loci compared to eSNPs or CREs alone. Given that eSNP- (Dimas et al., 2009; Fairfax et al., 2012; Gibbs et al., 2010; Nica et al., 2011) and CRE-mediated epigenetic regulation (Cheung et al., 2010; Heintzman et al., 2009; Maurano et al., 2012) is often specific for tissue and even cell type, our findings add to the growing evidence supporting the importance of studying the human brain tissue for functional genomics analysis in neuropsychiatric illnesses.

The strongest SCZ-associated enrichment was observed in fetal and adult brain creSNP annotations for enhancers. Previous studies have established the important regulatory role of the enhancers on transcriptome organization during neurodevelopment and adulthood (Andersson et al., 2014; Visel et al., 2013; Wenger et al., 2013). Overall, these findings suggest that risk-allele-specific alterations in enhancers could affect the proper spatiotemporal organization of the transcriptome that, when combined with other perturbations, leads to SCZ.

We have used a stepwise approach for defining functional enrichment and, in so doing, were led to a mechanistic hypothesis (of an interaction between disease signal, expression signal, and an enhancer) about the formation of chromosome loops between the enhancer and promoter. We experimentally validated these long-range interactions in human brain tissue and hiPSC-derived neurons for a gene that has been strongly associated with neuropsychiatric disorders. More specifically, *CACNA1C*,

a subunit of the L-type calcium channel, is one of the most widely reproduced associations, first identified in bipolar disorder (Psychiatric GWAS Consortium Bipolar Disorder Working Group, 2011; Ferreira et al., 2008; Sklar et al., 2008), but subsequently also shown to be strongly associated with SCZ (Ripke et al., 2013). The association signal is in the middle of an intron and does not suggest any immediate functional possibilities. In addition, the associated region is large (154.7 kb) and contains multiple implicated SNPs due to local LD patterns (216 SNPs with $p < 10^{-3}$). We have now demonstrated in postmortem human brain and hiPSC-derived neurons a specific interaction of a narrow, 1.4 kb region (which is an enhancer) with the proximal gene promoter by chromosome conformation capture. Furthermore, the risk variant is associated with reduced *CACNA1C* gene expression and transcriptional activity in the eSNP and in vitro experiments, respectively. Another recent study reported that *CACNA1C* rs1006737 (or rs2159100) is associated with decreased gene expression (Gershon et al., 2014), similar to our findings, although this is not consistently observed (Bigos et al., 2010). Since the initial report of *CACNA1C* association with bipolar disorder (Ferreira et al., 2008), there has been follow-up with studies that report effects on functional connectivity in attention and emotion networks, cognitive performance, and personality traits in SCZ and bipolar disorder (Bigos et al., 2010; Erk et al., 2010; Hori et al., 2012; Paulus et al., 2014; Radua et al., 2013; Roussos et al., 2011, 2013; Tesli et al., 2013).

Two out of the 17 genes identified through the RTC approach are calcium channels subunit genes (*CACNA1C* and *CACNB2*). We note that calcium channel subunits have been previously implicated in GWAS of bipolar disorder (Ferreira et al., 2008; Lee et al., 2011; Sklar et al., 2008; Psychiatric GWAS Consortium Bipolar Disorder Working Group, 2011), SCZ (Ripke et al., 2013), and cross-disorder analyses (Cross-Disorder Group of the Psychiatric Genomics Consortium, 2013). In addition, an enrichment of rare disruptive variants in calcium channel subunits was reported in a recent exome-sequencing study (Purcell et al.,

Table 2. Annotation of the 22 Genome-wide Significant Loci Using the Functional eSNP and CRE Data

SCZ GWAS			Recombination Interval		eSNP ^b	Distance (kb) ^c	RTC Analysis					
Chromosomal Region	Index SNP	p	Size (kb)	Genes ^a			r ²	Gene	RTC	Beta (SE) ^d	creSNP ^e	CRE
Chr. 6: 31,596,138–32,813,768	rs114002140	9.14 × 10 ⁻¹⁴	1,905.5	263 (127)	NA	–	–	–	–	–	–	–
Chr. 10: 104,487,871–105,245,420	rs7085104	3.68 × 10 ⁻¹³	4,807.9	135 (85)	rs4919690 ^f	12.4	0.64	AS3MT	1	-0.72 (0.07)	1	AP/DHS
					rs4919690 ^f	12.4	0.64	C10orf32	1	-0.51 (0.07)	1	AE/DHS
					rs56946876 ^f	24.7	0.68	NT5C2	0.98	-0.90 (0.04)	14	AP/AE/DHS
					rs619824 ^f	47.6	0.62	WBP1L	0.99	-0.64 (0.07)	–	–
Chr. 7: 1,827,717–2,346,115	rs6461049	5.93 × 10 ⁻¹³	3,196.4	66 (39)	rs12154473 ^f	35.3	0.85	SNX8	0.97	-0.34 (0.09)	–	–
Chr. 1: 98,141,112–98,664,991	rs1198588	1.72 × 10 ⁻¹²	775.5	24 (2)	rs1198572 ^f	55.7	0.87	RP11-490G2.2	0.98	-0.40 (0.08)	1	AE/DHS
Chr. 12: 2,285,731–2,440,464	rs1006737	5.22 × 10 ⁻¹²	1,339.0	61 (17)	rs758170 ^f	16.2	0.97	CACNA1C	1	-0.39 (0.09)	4	AE/DHS
Chr. 10: 18,601,928–18,934,390	rs17691888	1.27 × 10 ⁻¹⁰	882.1	36 (4)	rs10828653 ^f	38.2	0.59	CACNB2	1	-0.34 (0.08)	–	–
Chr. 8: 143,297,312–143,410,423	rs4129585	2.19 × 10 ⁻¹⁰	538.9	68 (16)	rs11988625	7.4	0.52	LYPD2	0.89	0.33 (0.09)	NA	NA
Chr. 1: 73,275,828–74,099,273	rs10789369	3.64 × 10 ⁻¹⁰	1,814.3	33 (3)	rs10890066	346.9	0.002	CRYZ	0.48	0.30 (0.08)	NA	NA
Chr. 11: 130,706,918–130,894,976	rs7940866	1.83 × 10 ⁻⁹	240.4	34 (7)	rs10791107	28.9	0.78	APLP2	0.88	0.36 (0.09)	NA	NA
Chr. 5: 151,888,959–152,835,304	rs17504622	2.65 × 10 ⁻⁹	1,242.4	34 (9)	NA	–	–	–	–	–	–	–
Chr. 19: 19,354,937–19,744,079	rs2905424	3.44 × 10 ⁻⁹	7,682.3	321 (160)	rs7254230 ^f	39.1	0.91	GATAD2A	1	-0.38 (0.08)	14	AP/AE/DHS
					rs2074295 ^f	104.0	0.45	GMIP	0.99	0.32 (0.08)	–	–
					rs12460764 ^f	41.5	0.91	HAPLN4	1	0.34 (0.08)	14	AP/AE/DHS
Chr. 2: 37,422,072–37,592,628	rs2373000 ^g	6.78 × 10 ⁻⁹	666.1	32 (13)	rs12621276	293.5	0.06	EIF2AK2	0.89	-0.40 (0.09)	NA	NA
Chr. 5: 101,581,848–101,870,822	rs6878284 ^g	9.03 × 10 ⁻⁹	3,643.4	42 (8)	NA	–	–	–	–	–	–	–
Chr. 3: 52,215,002–53,175,017	rs4687552	1.16 × 10 ⁻⁸	7,777.1	294 (142)	rs12486554 ^f	95.9	0.75	GNL3	0.99	-0.40 (0.08)	15	AP/AE/DHS
					rs2268023 ^f	19.1	0.78	NEK4	0.95	-0.28 (0.07)	13	AP/AE/DHS
					rs13071584 ^f	33.9	0.74	SPCS1	0.99	0.34 (0.08)	14	AP/AE/DHS

(Continued on next page)

Table 2. Continued

SCZ GWAS			Recombination Interval				RTC Analysis					
Chromosomal Region	Index SNP	p	Size (kb)	Genes ^a	eSNP ^b	Distance (kb) ^c	r ²	Gene	RTC	Beta (SE) ^d	creSNP ^e	CRE
Chr. 2: 145,139,727–145,214,607	rs12991836	1.19 × 10 ⁻⁸	1,164.0	29 (5)	rs72858496	68.4	0.01	GTDC1	0.8	0.38 (0.08)	NA	NA
Chr. 2: 200,628,118–201,293,421	rs2949006	1.21 × 10 ⁻⁸	1,916.3	61 (18)	rs35220450 ^f	65.3	0.83	TYW5	0.98	-0.52 (0.07)	3	AP/AE/DHS
Chr. 18: 52,722,378–52,827,668	rs4801131	1.22 × 10 ⁻⁸	1,047.2	33 (10)	rs8084537	121.7	0.002	TCF4	0.15	-0.33 (0.08)	NA	NA
Chr. 2: 233,550,961–233,808,241	rs778371	1.51 × 10 ⁻⁸	1,945.1	105 (42)	rs778371	0.0	-	NGEF	1	0.56 (0.07)	7	AE
Chr. 1: 243,593,066–244,025,999	rs14403	1.80 × 10 ⁻⁸	1,614.2	51 (11)	rs3006916 ^f	24.0	0.64	SDCCAG8	0.98	0.42 (0.09)	3	AE/DHS
Chr. 12: 123,447,928–123,913,433	rs11532322	2.28 × 10 ⁻⁸	2,236.6	101 (50)	NA	-	-	-	-	-	-	-
Chr. 1: 243,418,063–243,627,135	rs1538774	2.53 × 10 ⁻⁸	1,614.2	51 (11)	rs3006916	95.0	0.02	SDCCAG8	0.57	0.42 (0.09)	NA	NA
Chr. 8: 89,188,454–89,761,163	rs11995572	3.33 × 10 ⁻⁸	1,550.2	24 (7)	NA	-	-	-	-	-	-	-
Chr. 5: 60,484,179–60,843,706	rs171748	3.78 × 10 ⁻⁸	2,761.2	48 (14)	rs295571	72.1	0.20	PDE4D	0.87	0.31 (0.08)	NA	NA
Chr. 5: 152,505,453–152,707,306	rs2910032	4.12 × 10 ⁻⁸	1,242.4	34 (9)	rs2118792	30.2	0.07	FAM114A2	0.88	0.37 (0.08)	NA	NA

AE, active enhancer; AP, active promoter; DHS, DNase I hypersensitive site; RTC, regulatory trait concordance.

^aNumber of genes (based on the Gencode v16 annotations) that lie within 1 Mb upstream or downstream from recombination intervals. In parentheses are the numbers of genes that were affected by eSNPs and included in the RTC analysis for each recombination interval.

^beSNP with the highest RTC score for each SCZ GWAS chromosomal region. NA indicates that the GWAS SNP was excluded from the eSNP analysis due to MAF < 5% (rs17504622) or increased missingness (>10%) per marker after imputation (rs6878284, rs114002140, rs11532322, and rs11995572).

^cDistance among the eSNP and index SCZ GWAS SNP.

^dStandardized beta coefficient and SE for the effect of minor allele on gene expression.

^eNumber of creSNPs that are in strong LD (within 500 kb and with r² > 0.8) with the eSNP.

^feSNPs with RTC ≥ 0.9. For GWAS regions with no eSNP at RTC ≥ 0.9, we present the eSNP with the highest RTC. For those SNP, no creSNP or CRE data are presented.

^gThis region was not genome-wide significant in the recent PGC2 GWAS analysis (Schizophrenia Working Group of the Psychiatric Genomics Consortium, 2014).

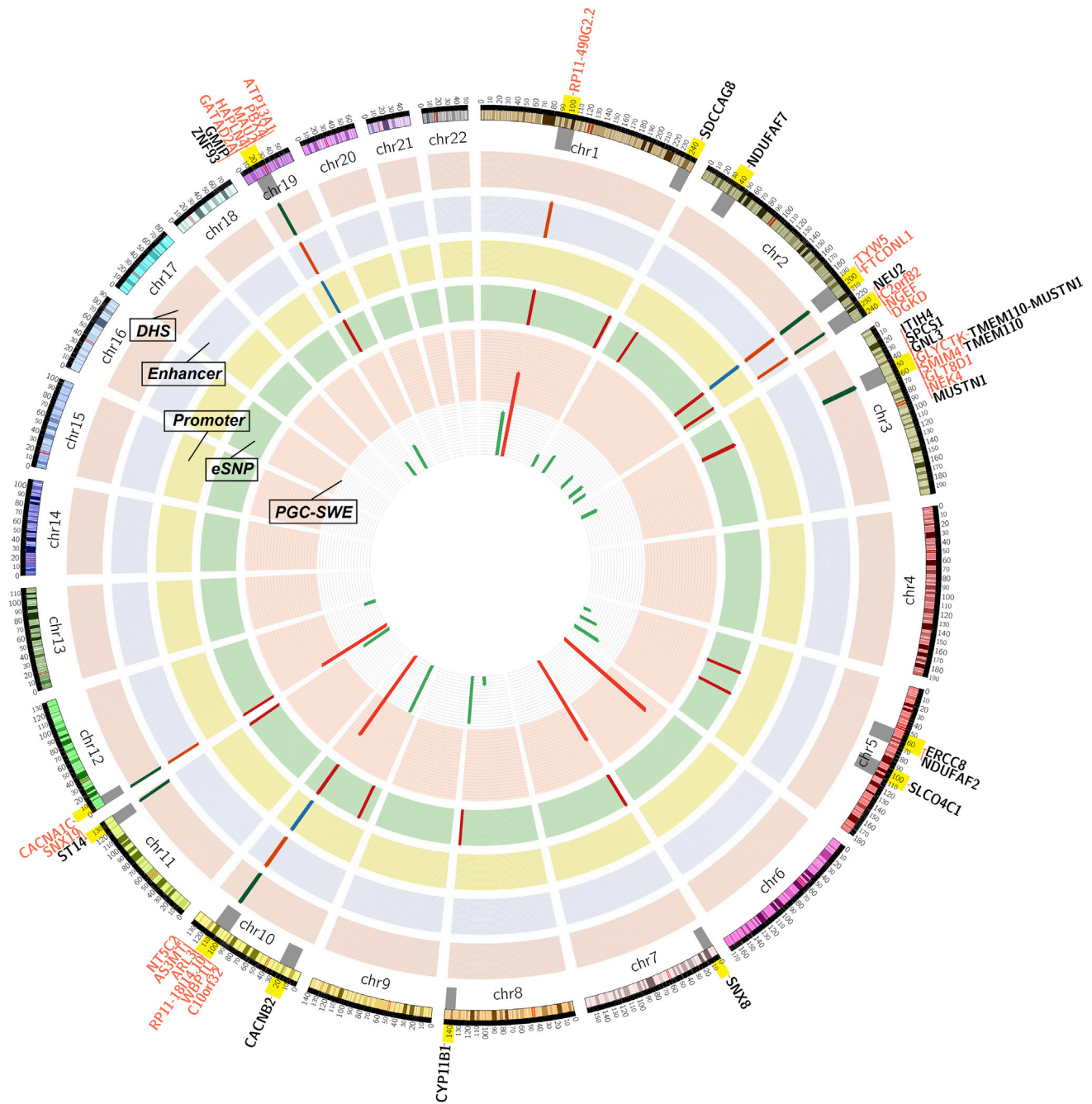


Figure 4. Functional Genomic Analysis for the SCZ Genome-wide Significant Loci

Layer 1 shows the 24 genome-wide significant loci. Green lines illustrate loci with $-\log_{10} p$ value ≤ 10 , and red lines show loci with $-\log_{10} p$ value > 10 . Layer 2 (eSNP) illustrates which of the 24 significant loci had eSNP with $RTC \geq 0.9$. Layers 3–5 show whether eSNPs (and tag SNPs with $r^2 > 0.8$ within 500 kb) lie within active promoter (layer 3; promoter), active enhancer (layer 4; enhancer), or DNase I hypersensitive site (layer 5; DHS). Genes affected by functional SNPs are illustrated outside the circo. In black fonts are genes affected by eSNP. In red fonts are genes affected by creSNPs (within active promoter, active enhancer, or DHS).

2014). *CACNA1C* codes for $Ca_v1.2$, the most abundant neuronal L-type calcium channel (Obermair et al., 2004). The α_{1c} subunit (*CACNA1C*) forms the transmembrane pore and directly interacts with the intracellular β_2 subunit (*CACNB2*). The cytosolic β_2 subunit has a major role in stabilizing the α_1 subunit conforma-

tion and delivering it to the cell membrane by its ability to mask an ER retention signal in the α_1 subunit (Bichet et al., 2000). Calcium-mediated signaling has an important role on neuronal differentiation by regulating axonal growth and guidance, and this process is also controlled by glutamatergic signaling

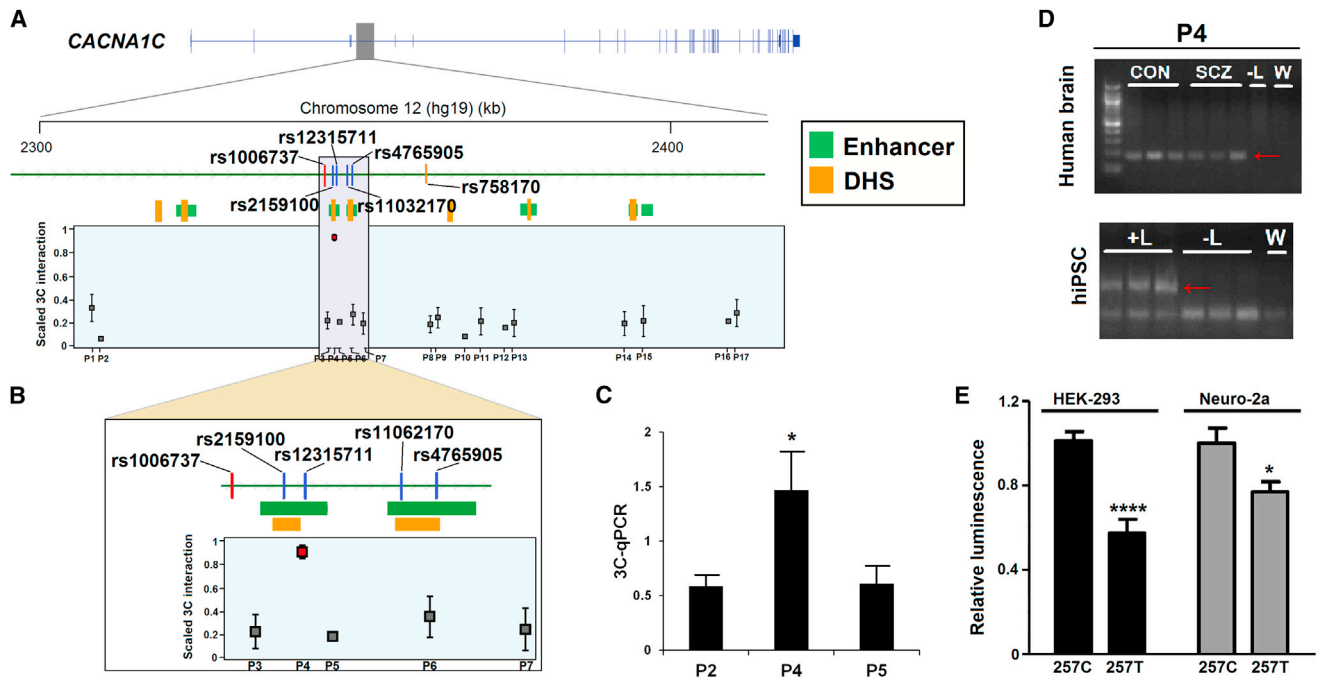


Figure 5. A Physical Interaction between the *CACNA1C* Promoter and an Enhancer Region Was Confirmed by 3C

(A) Part of the genomic region of *CACNA1C* (chr12: 2,303,497–2,419,832) is displayed. The index SNP (red line; rs1006737), eSNP (orange line; rs758170), and tag SNPs (blue line; $r^2 > 0.8$ within 500 kb) that lie within CREs (enhancer and DHS) are illustrated. The index SNP and SNPs in LD with them are associated with lower *CACNA1C* gene expression. 3C-PCR primers were designed at the *CACNA1C* TSSs and multiple regions (primers nos. 1–17). A 3C physical interaction between the *CACNA1C* TSS and primer no. 4 was found in 3C libraries made from postmortem brain tissue (n = 6; F [16, 83] = 5.52; p = 8×10^{-8}).

(B) More detailed view of the associated region (chr12: 2,344,353–2,362,387). The primer no. 4 includes the rs2159100 creSNP (GWAS p value = 1.1×10^{-10}), which lies within an active enhancer (green box) and DHS (orange box).

(C) 3C-qPCR shows increased interaction for primer no. 4 in libraries made from postmortem brain tissue (n = 6; F [2, 15] = 4.54; p = 0.029).

(D) Gel images are shown for primer no. 4 for 3C interactions using prefrontal cortex libraries in controls and SCZ- and hiPSC-derived neurons. The red arrow shows the 3C interaction band. All 3C PCR products were sequence verified, and the interactions were not present in the no ligase (-L) and water (W) controls.

(E) The rs2159100 T risk allele (position 257 in the construct: 257T) affects the relative luciferase activity in HEK293 and Neuro-2a cells compared to the C allele (257C).

Data show the mean and SEM. *p < 0.05 and ****p < 0.0001 by unpaired t test.

(Rosenberg and Spitzer, 2011). It is possible that altered tuning in calcium-mediated signaling triggered by $Ca_v1.2$ and glutamatergic neurotransmission (Fromer et al., 2014; Purcell et al., 2014) could lead to alterations in the rate of axon outgrowth and pathfinding, resulting in inefficient neuronal wiring in SCZ.

Whereas our approach can identify functional categories with higher enrichment compared to FUV categories, we still observe a deviation from the null for the FUV category, indicating multiple SCZ-associated loci that were not captured through our current functional annotation categories. Clearly, current databases do not yet capture all types of functional variants, including sites of DNA methylation and hydroxymethylation (Lister et al., 2013), as well as additional CREs such as insulators (Herold et al., 2012). Furthermore, there is relatively low genomic resolution of current functional categories and many additional alternative putative mechanisms, such as transcriptional regulation through small and long noncoding RNAs and alternative splicing, likely mediate the effect of some noncoding risk alleles.

In conclusion, these results suggest a tissue-specific regulatory role for many SCZ-associated common loci. While this paper was under review, a mega-analysis by the Psychiatric

Genomic Consortium (PGC) in SCZ on over 80,000 cases and controls was published (Schizophrenia Working Group of the Psychiatric Genomics Consortium, 2014). In the new PGC GWAS, 22 out of 24 loci remain genome-wide significant. In addition, 19 out of the 24 SNPs presented in Table 2 were in LD ($r^2 \geq 0.3$) with a genome-wide significant PGC index SNP. Our analysis provides a framework for future integrative analysis of additional data sets to generate testable hypotheses and derive mechanistic insights for SCZ-associated variants.

EXPERIMENTAL PROCEDURES

A brief description of key methods and sample description are provided below, whereas complete details are found in the Supplemental Experimental Procedures.

GWAS Data Sets

A large published SCZ GWAS data set (Ripke et al., 2013) in the form of summary statistic p values was obtained from public access website (<http://www.med.unc.edu/pgc/>). A previously published GWAS data set in rheumatoid arthritis (Stahl et al., 2010) was obtained through collaboration with investigators in the form of summary statistic p values. For all the analyses

presented here, the MHC locus (chr6: 25–35 Mb) was excluded from both GWAS data sets.

eSNP Data Sets

Brain eSNPs were generated using the gene expression and genotyping data of Caucasian samples, included in the Braincloud (Colantuoni et al., 2011; Gene Expression Omnibus [GEO] accession number: GSE30272), NIA/NIH (Gibbs et al., 2010; GEO accession number: GSE15745), and Harvard Brain Tissue Resource Center (Zhang et al., 2014; GEO accession number: GSE44772) data sets (Table S1). The following nonbrain eSNP data sets were downloaded from public access websites: LCL (Xia et al., 2012; http://www.bios.unc.edu/research/genomic_software/seeQTL/), liver (Innocenti et al., 2011; <http://www.scandb.org/>), PBMCs (Westra et al., 2013; <http://genenetwork.nl/bloodseqtlbrowser/>), skin (Grundberg et al., 2012), and adipose tissue (Grundberg et al., 2012; <http://www.muther.ac.uk/Data.html>).

cis-Regulatory Element Annotations

Multiple CRE annotations were used in the current study (Tables S2 and S3). ChIP-seq and DHS data generated as part of the ENCODE (Maurano et al., 2012) and REMC (Zhu et al., 2013) projects for human brain/neuron (Table S2), T-helper cells, liver, skin, and adipose tissue were downloaded from the National Center for Biotechnology Information repository (<http://www.ncbi.nlm.nih.gov/geo/roadmap/epigenomics/>). Additional data for the dorsolateral prefrontal cortex after fluorescence-activated cell sorting were generated as described previously (Cheung et al., 2010; Shulha et al., 2012, 2013; Table S3).

Definition of Functional Data Sets

All SNP coordinates described here are relative to UCSC hg19. The functional data sets used in the current study were divided into three groups: eSNP, CRE and creSNP (eSNP in a cis-regulatory element).

- (1) eSNP: the brain eSNP data set was generated by including all significant cis eSNPs derived from each eSNP analysis. For the nonbrain eSNPs (LCL, liver, skin, PBMCs, and adipose tissue), we used the list of cis eSNPs generated as described previously (Grundberg et al., 2012; Innocenti et al., 2011; Westra et al., 2013; Xia et al., 2012) at FDR 10%.
- (2) CRE: the ChIP-seq and DHS significant peaks were clustered into subgroups based on assay and origin of tissue (Figure S4). We integrated multiple CRE subgroup annotations for generating functional annotations defining active promoters (overlap of H3K4me3 with H3K9ac or H3K27ac), poised promoters (overlap of H3K4me3 with H3K27me3), active enhancers (overlap of H3K4me3 with H3K9ac or H3K27ac), repressed enhancers (overlap of H3K4me1 with H3K27me3), and open chromatin (DHS).
- (3) creSNP: the creSNP functional data set was defined as the eSNPs that lie within different CRE subcategories.

GWAS Positional Annotation

We used a mixed approach for assigning the GWAS SNPs into functional categories. For the eSNP functional category, we leveraged the eSNP data set in the densely mapped 1000G to identify the GWAS studied SNP that was tagged, as a result of LD. For generating the CRE or creSNP functional categories, we used a positional approach (ignoring the annotation categories of SNPs in LD with the tag SNP). This mixed model allows us to capture all possible SNPs that affect gene expression (tag or SNPs in LD), followed by positional selection of SNPs that lie within putative regulatory DNA regions. GWAS SNP that did not fit in any functional category was assigned as the FUV category. The Table S4 describes the count of SCZ for each functional brain category.

Quantification of Enrichment

Stratified Q-Q plots were generated for assessment of the similarity or differences between the empirical cumulative distribution function of the functional and FUV data sets. In the stratified Q-Q plots, the enrichment of SCZ SNPs for a specific functional category is observed as a horizontal deflection from the FUV category. The quantification of enrichment for each functional category

was done using the CES (mean $[z^2 - 1]$), as described previously (Schork et al., 2013). The CES provides a summary score of category-specific enrichment where the mean is taken over all SNP Z scores in the given category. For each functional category, the statistical significance of CES was evaluated by permutation on a combined 10,000 randomized set of CREs and eSNPs.

Regulatory Trait Concordance Score

The likelihood of a shared functional effect between a SCZ genome-wide significant SNP and an eSNP was assessed by the RTC approach (Grundberg et al., 2012; Nica et al., 2010). RTC score ranges from 0 to 1, with values ≥ 0.9 indicating the GWAS signal and eSNP tag the same underlying signal, as demonstrated previously (Grundberg et al., 2012; Nica et al., 2010).

Chromosome Conformation Capture

Postmortem prefrontal cortex brain tissue for cases with SCZ and controls was obtained from the University of Maryland and pair matched for age, sex, postmortem interval, and pH ($n = 3$ /group; Table S8). Chromosome conformation capture (3C) was performed as described in a recently published protocol applicable to postmortem brain (Mitchell et al., 2014). Physical looping interactions were quantified with PCR. Primers were designed less than 120 bp from the HindIII or NcoI restriction site (Table S9). The PCR products were resolved on a 2% agarose gel, and the level of interaction between two primers was measured semiquantitatively using band intensities normalized with the background (raw 3C interaction) with ImageJ (Schneider et al., 2012). For each library (HindIII and NcoI) in the human postmortem brain tissue studies, we transformed the raw 3C interaction to Z scores, followed by scaling (0 to 1; scaled 3C interaction). All 3C PCR products were sequence verified, and the interactions were not present in the no ligase and water controls. For primers no. 2, no. 4, and no. 5, physical looping interactions were further quantified with quantitative PCR (qPCR) using an ABI Prism 7900 (Applied Biosystems). The reactions were run in triplicate for each sample, and DNA PCR product was measured through SYBR Green I (Life Technologies).

Human Induced Pluripotent Stem Cells Differentiation to Neurons

hiPSCs were derived from fibroblasts of a control sample (GM03651) as described previously (Brennand et al., 2011). hiPSC-derived neurons were differentiated for ~6 weeks in neural differentiation media. The majority of forebrain hiPSC neurons are VGLUT1-positive and so are presumably glutamatergic, although approximately 30% of neurons are GAD67-positive (GABAergic; Brennand et al., 2011).

Transient Transfection and Luciferase Assays

We constructed luciferase reporter plasmids by cloning the regulatory sequence containing rs2159100 into the pGL4.24 vector (Promega) upstream of the minP. HEK293 cells or Neuro-2a cells (40%–60% confluent) were transfected with each construct (500 ng) and the Renilla luciferase expression vector pRL-TK (200 ng; Promega). The luciferase activity in the cell lysates was determined using the Dual Luciferase Reporter System (Promega). Firefly luciferase activities were normalized to that of Renilla luciferase, and expression relative to the activity of the rs2159100 C allele was noted.

ACCESSION NUMBERS

The GEO accession number for the H3K4me3 ChIP-seq data reported in this paper (Table S3) is GSE62391.

SUPPLEMENTAL INFORMATION

Supplemental Information includes Supplemental Experimental Procedures, five figures, and nine tables and can be found with this article online at <http://dx.doi.org/10.1016/j.celrep.2014.10.015>.

AUTHOR CONTRIBUTIONS

P.R., E.E.S., S.A., and P.S. designed and supervised the research. P.R., E.A.S., D.M.R., A.C., M.F., and S.M.P. performed the statistical analysis.

A.C.M., J.F.F., V.M.P., J.T., and S.A. performed the chromatin conformation capture experiments. G.V., A.G., and N.K.R. performed the luciferase assay. K.B. generated the hiPSCs. Y.O., K.A.S., J.W., L.P., L.K., P.K.G., R.M.P., and S.R. provided the GWAS in rheumatoid arthritis. P.R., S.A., and P.S. prepared the manuscript. P.R. and A.C.M. contributed equally to this work.

ACKNOWLEDGMENTS

We thank Iris Cheung and Yin Guo for ChIP-seq assays on sorted brain nuclei. We thank all members of the Rheumatoid Arthritis Consortium for providing access to the GWAS data. Members of Rheumatoid Arthritis Consortium are Steve Eyre, John Bowes, Dorothee Diogo, Annette Lee, Anne Barton, Paul Martin, Alexandra Zhermakova, E.A.S., Sebastien Viatte, Kate McAllister, Christopher I. Amos, L.P., Rene E. M. Toes, Tom W. J. Huizinga, Cisca Wijmenga, Gosia Trynka, Lude Franke, Harm-Jan Westra, Lars Alfredsson, Xinli Hu, Cynthia Sandor, Paul I. W. de Bakker, Sonia Davila, Chiea Chuen Khor, Khai Koon Heng, Robert Andrews, Sarah Edkins, Sarah E. Hunt, Cordelia Langford, Deborah Symmons, Biologics in Rheumatoid Arthritis Genetics and Genomics Study Syndicate, Wellcome Trust Case Control Consortium, Pat Concannon, Suna Onengut-Gumuscu, Stephen S. Rich, Panos Deloukas, Miguel A. Gonzalez-Gay, Luis Rodriguez-Rodriguez, Lisbeth Árisetig, Javier Martin, Solbritt Rantapää-Dahlqvist, R.M.P., S.R., L.K., P.K.G., J.W., the Biologics in Rheumatoid Arthritis Genetics and Genomics Study Syndicate (BRAGSS), and the Wellcome Trust Case Control Consortium (WTCCC). We thank Dr. Ron Zielke and staff from the Brain and Tissue Bank for Developmental Disorders, and Dr. Andree Lessard from the Maryland Psychiatric Research Center, University of Maryland, for providing postmortem brain tissue. We acknowledge funding support from NIH/National Institute of Mental Health (NIMH) grant R01MH095034 (to P.S.), NIMH grant R01MH097276 (to P.S. and E.E.S.), NIMH grant U01MH103392 (to S.A. and P.S.), NIMH grant P50 MH096890 (to S.A.), National Institute of Neurological Disorders and Stroke (NINDS) grant R21 NS076958 (to S.A.), NINDS grant R01 NS047229 (to N.K.R.), National Institute on Aging (NIA) grant R37 AG017926 (to N.K.R.), NIA grant P50 AG005138 (to N.K.R. and A.G.), Veterans Affairs Merit grant BX002395 (to P.R.), the Brain Behavior Research Foundation (to P.R., A.C.M., S.A., E.A.S., and K.B.), the American Psychiatric Association-Merck & Co. Early Academic Career Research Award (to P.R.), NIMH grant R01 MH101454 (to K.B.), the New York Stem Cell Foundation (to K.B.), Alzheimer's Association grant IIRG-11-205149 (to A.G.), the Friedman Brain Institute at Icahn School of Medicine at Mount Sinai, and the Icahn Institute for Genomics and Multiscale Biology at Icahn School of Medicine at Mount Sinai. This work was supported in part through the computational resources and staff expertise provided by the Department of Scientific Computing at the Icahn School of Medicine at Mount Sinai. The funders had no role in study design, execution, analysis, or manuscript preparation.

Received: May 24, 2014

Revised: July 31, 2014

Accepted: October 3, 2014

Published: November 6, 2014

REFERENCES

- Andersson, R., Gebhard, C., Miguel-Escalada, I., Hoof, I., Bornholdt, J., Boyd, M., Chen, Y., Zhao, X., Schmidl, C., Suzuki, T., et al.; FANTOM Consortium (2014). An atlas of active enhancers across human cell types and tissues. *Nature* **507**, 455–461.
- Bichet, D., Cornet, V., Geib, S., Carlier, E., Volsen, S., Hoshi, T., Mori, Y., and De Waard, M. (2000). The I-II loop of the Ca²⁺ channel alpha1 subunit contains an endoplasmic reticulum retention signal antagonized by the beta subunit. *Neuron* **25**, 177–190.
- Bigos, K.L., Mattay, V.S., Callicott, J.H., Straub, R.E., Vakkalanka, R., Kolachana, B., Hyde, T.M., Lipska, B.K., Kleinman, J.E., and Weinberger, D.R. (2010). Genetic variation in CACNA1C affects brain circuitries related to mental illness. *Arch. Gen. Psychiatry* **67**, 939–945.
- Brennan, K.J., Simone, A., Jou, J., Gelboin-Burkhardt, C., Tran, N., Sangar, S., Li, Y., Mu, Y., Chen, G., Yu, D., et al. (2011). Modelling schizophrenia using human induced pluripotent stem cells. *Nature* **473**, 221–225.
- Cheung, I., Shulha, H.P., Jiang, Y., Matevossian, A., Wang, J., Weng, Z., and Akbarian, S. (2010). Developmental regulation and individual differences of neuronal H3K4me3 epigenomes in the prefrontal cortex. *Proc. Natl. Acad. Sci. USA* **107**, 8824–8829.
- Colantuoni, C., Lipska, B.K., Ye, T., Hyde, T.M., Tao, R., Leek, J.T., Colantuoni, E.A., Elkahlon, A.G., Herman, M.M., Weinberger, D.R., and Kleinman, J.E. (2011). Temporal dynamics and genetic control of transcription in the human prefrontal cortex. *Nature* **478**, 519–523.
- Cross-Disorder Group of the Psychiatric Genomics Consortium (2013). Identification of risk loci with shared effects on five major psychiatric disorders: a genome-wide analysis. *Lancet* **381**, 1371–1379.
- Degner, J.F., Pai, A.A., Pique-Regi, R., Veyrieras, J.B., Gaffney, D.J., Pickrell, J.K., De Leon, S., Michelini, K., Lewellen, N., Crawford, G.E., et al. (2012). DNase I sensitivity QTLs are a major determinant of human expression variation. *Nature* **482**, 390–394.
- Dimas, A.S., Deutsch, S., Stranger, B.E., Montgomery, S.B., Borel, C., Attar-Cohen, H., Ingle, C., Beazley, C., Gutierrez Arcelus, M., Sekowska, M., et al. (2009). Common regulatory variation impacts gene expression in a cell type-dependent manner. *Science* **325**, 1246–1250.
- Erk, S., Meyer-Lindenberg, A., Schnell, K., Opitz von Boberfeld, C., Esslinger, C., Kirsch, P., Grimm, O., Arnold, C., Haddad, L., Witt, S.H., et al. (2010). Brain function in carriers of a genome-wide supported bipolar disorder variant. *Arch. Gen. Psychiatry* **67**, 803–811.
- Fairfax, B.P., Makino, S., Radhakrishnan, J., Plant, K., Leslie, S., Dilthey, A., Ellis, P., Langford, C., Vannberg, F.O., and Knight, J.C. (2012). Genetics of gene expression in primary immune cells identifies cell type-specific master regulators and roles of HLA alleles. *Nat. Genet.* **44**, 502–510.
- Fanucchi, S., Shibayama, Y., Burd, S., Weinberg, M.S., and Mhlanga, M.M. (2013). Chromosomal contact permits transcription between coregulated genes. *Cell* **155**, 606–620.
- Ferreira, M.A., O'Donovan, M.C., Meng, Y.A., Jones, I.R., Ruderfer, D.M., Jones, L., Fan, J., Kirov, G., Perlis, R.H., Green, E.K., et al.; Wellcome Trust Case Control Consortium (2008). Collaborative genome-wide association analysis supports a role for ANK3 and CACNA1C in bipolar disorder. *Nat. Genet.* **40**, 1056–1058.
- Fromer, M., Pocklington, A.J., Kavanagh, D.H., Williams, H.J., Dwyer, S., Gormley, P., Georgieva, L., Rees, E., Palta, P., Ruderfer, D.M., et al. (2014). De novo mutations in schizophrenia implicate synaptic networks. *Nature* **506**, 179–184.
- Gershon, E.S., Grennan, K., Busnello, J., Badner, J.A., Ovsiew, F., Memon, S., Alliey-Rodriguez, N., Cooper, J., Romanos, B., and Liu, C. (2014). A rare mutation of CACNA1C in a patient with bipolar disorder, and decreased gene expression associated with a bipolar-associated common SNP of CACNA1C in brain. *Mol. Psychiatry* **19**, 890–894.
- Gibbs, J.R., van der Brug, M.P., Hernandez, D.G., Traynor, B.J., Nalls, M.A., Lai, S.L., Arepalli, S., Dillman, A., Rafferty, I.P., Troncoso, J., et al. (2010). Abundant quantitative trait loci exist for DNA methylation and gene expression in human brain. *PLoS Genet.* **6**, e1000952.
- Grundberg, E., Small, K.S., Hedman, A.K., Nica, A.C., Buil, A., Keildson, S., Bell, J.T., Yang, T.P., Meduri, E., Barrett, A., et al.; Multiple Tissue Human Expression Resource (MuTHER) Consortium (2012). Mapping cis- and trans-regulatory effects across multiple tissues in twins. *Nat. Genet.* **44**, 1084–1089.
- Harismendy, O., Notani, D., Song, X., Rahim, N.G., Tanasa, B., Heintzman, N., Ren, B., Fu, X.D., Topol, E.J., Rosenfeld, M.G., and Frazer, K.A. (2011). 9p21 DNA variants associated with coronary artery disease impair interferon- γ signaling response. *Nature* **470**, 264–268.
- Heintzman, N.D., Hon, G.C., Hawkins, R.D., Kheradpour, P., Stark, A., Harp, L.F., Ye, Z., Lee, L.K., Stuart, R.K., Ching, C.W., et al. (2009). Histone modifications at human enhancers reflect global cell-type-specific gene expression. *Nature* **459**, 108–112.

- Herold, M., Bartkuhn, M., and Renkawitz, R. (2012). CTCF: insights into insulator function during development. *Development* 139, 1045–1057.
- Hori, H., Yamamoto, N., Fujii, T., Teraishi, T., Sasayama, D., Matsuo, J., Kawamoto, Y., Kinoshita, Y., Ota, M., Hattori, K., et al. (2012). Effects of the CACNA1C risk allele on neurocognition in patients with schizophrenia and healthy individuals. *Sci. Rep.* 2, 634.
- Innocenti, F., Cooper, G.M., Stanaway, I.B., Gamazon, E.R., Smith, J.D., Mirkov, S., Ramirez, J., Liu, W., Lin, Y.S., Moloney, C., et al. (2011). Identification, replication, and functional fine-mapping of expression quantitative trait loci in primary human liver tissue. *PLoS Genet.* 7, e1002078.
- Kagey, M.H., Newman, J.J., Bilodeau, S., Zhan, Y., Orlando, D.A., van Berkum, N.L., Ebmeier, C.C., Goossens, J., Rahl, P.B., Levine, S.S., et al. (2010). Mediator and cohesin connect gene expression and chromatin architecture. *Nature* 467, 430–435.
- Lee, M.T., Chen, C.H., Lee, C.S., Chen, C.C., Chong, M.Y., Ouyang, W.C., Chiu, N.Y., Chuo, L.J., Chen, C.Y., Tan, H.K., et al. (2011). Genome-wide association study of bipolar I disorder in the Han Chinese population. *Mol. Psychiatry* 16, 548–556.
- Lister, R., Mukamel, E.A., Nery, J.R., Urich, M., Puddifoot, C.A., Johnson, N.D., Lucero, J., Huang, Y., Dwork, A.J., Schultz, M.D., et al. (2013). Global epigenomic reconfiguration during mammalian brain development. *Science* 341, 1237905.
- Maurano, M.T., Humbert, R., Rynes, E., Thurman, R.E., Haugen, E., Wang, H., Reynolds, A.P., Sandstrom, R., Qu, H., Brody, J., et al. (2012). Systematic localization of common disease-associated variation in regulatory DNA. *Science* 337, 1190–1195.
- Mitchell, A.C., Bharadwaj, R., Whittle, C., Krueger, W., Mirics, K., Hurd, Y., Rasmussen, T., and Akbarian, S. (2014). The genome in three dimensions: a new frontier in human brain research. *Biol. Psychiatry* 75, 961–969.
- Musunuru, K., Strong, A., Frank-Kamenetsky, M., Lee, N.E., Ahfeldt, T., Sachs, K.V., Li, X., Li, H., Kuperwasser, N., Ruda, V.M., et al. (2010). From noncoding variant to phenotype via SORT1 at the 1p13 cholesterol locus. *Nature* 466, 714–719.
- Nica, A.C., Montgomery, S.B., Dimas, A.S., Stranger, B.E., Beazley, C., Barroso, I., and Dermitzakis, E.T. (2010). Candidate causal regulatory effects by integration of expression QTLs with complex trait genetic associations. *PLoS Genet.* 6, e1000895.
- Nica, A.C., Parts, L., Glass, D., Nisbet, J., Barrett, A., Sekowska, M., Travers, M., Potter, S., Grundberg, E., Small, K., et al.; MuTHER Consortium (2011). The architecture of gene regulatory variation across multiple human tissues: the MuTHER study. *PLoS Genet.* 7, e1002003.
- Nicolae, D.L., Gamazon, E., Zhang, W., Duan, S., Dolan, M.E., and Cox, N.J. (2010). Trait-associated SNPs are more likely to be eQTLs: annotation to enhance discovery from GWAS. *PLoS Genet.* 6, e1000888.
- Obermair, G.J., Szabo, Z., Bourinet, E., and Flucher, B.E. (2004). Differential targeting of the L-type Ca²⁺ channel alpha 1C (CaV1.2) to synaptic and extrasynaptic compartments in hippocampal neurons. *Eur. J. Neurosci.* 19, 2109–2122.
- Okada, Y., Wu, D., Trynka, G., Raj, T., Terao, C., Ikari, K., Kochi, Y., Ohmura, K., Suzuki, A., Yoshida, S., et al.; RACI consortium; GARNET consortium (2014). Genetics of rheumatoid arthritis contributes to biology and drug discovery. *Nature* 506, 376–381.
- Paulus, F.M., Bedenbender, J., Krach, S., Pyka, M., Krug, A., Sommer, J., Mette, M., Nöthen, M.M., Witt, S.H., Rietschel, M., et al. (2014). Association of rs1006737 in CACNA1C with alterations in prefrontal activation and fronto-hippocampal connectivity. *Hum. Brain Mapp.* 35, 1190–1200.
- Psychiatric GWAS Consortium Bipolar Disorder Working Group (2011). Large-scale genome-wide association analysis of bipolar disorder identifies a new susceptibility locus near ODZ4. *Nat. Genet.* 43, 977–983.
- Purcell, S.M., Moran, J.L., Fromer, M., Ruderfer, D., Solovieff, N., Roussos, P., O'Dushlaine, C., Chambert, K., Bergen, S.E., Kähler, A., et al. (2014). A polygenic burden of rare disruptive mutations in schizophrenia. *Nature* 506, 185–190.
- Radua, J., Surguladze, S.A., Marshall, N., Walshe, M., Bramon, E., Collier, D.A., Prata, D.P., Murray, R.M., and McDonald, C. (2013). The impact of CACNA1C allelic variation on effective connectivity during emotional processing in bipolar disorder. *Mol. Psychiatry* 18, 526–527.
- Richards, A.L., Jones, L., Moskvina, V., Kirov, G., Gejman, P.V., Levinson, D.F., Sanders, A.R., Purcell, S., Visscher, P.M., Craddock, N., et al.; Molecular Genetics of Schizophrenia Collaboration (MGS); International Schizophrenia Consortium (ISC) (2012). Schizophrenia susceptibility alleles are enriched for alleles that affect gene expression in adult human brain. *Mol. Psychiatry* 17, 193–201.
- Ripke, S., O'Dushlaine, C., Chambert, K., Moran, J.L., Kähler, A.K., Akterin, S., Bergen, S.E., Collins, A.L., Crowley, J.J., Fromer, M., et al.; Multicenter Genetic Studies of Schizophrenia Consortium; Psychosis Endophenotypes International Consortium; Wellcome Trust Case Control Consortium 2 (2013). Genome-wide association analysis identifies 13 new risk loci for schizophrenia. *Nat. Genet.* 45, 1150–1159.
- Rosenberg, S.S., and Spitzer, N.C. (2011). Calcium signaling in neuronal development. *Cold Spring Harb. Perspect. Biol.* 3, a004259.
- Roussos, P., Giakoumaki, S.G., Georgakopoulos, A., Robakis, N.K., and Bitsios, P. (2011). The CACNA1C and ANK3 risk alleles impact on affective personality traits and startle reactivity but not on cognition or gating in healthy males. *Bipolar Disord.* 13, 250–259.
- Roussos, P., Bitsios, P., Giakoumaki, S.G., McClure, M.M., Hazlett, E.A., New, A.S., and Siever, L.J. (2013). CACNA1C as a risk factor for schizotypal personality disorder and schizotypy in healthy individuals. *Psychiatry Res.* 206, 122–123.
- Schizophrenia Working Group of the Psychiatric Genomics Consortium (2014). Biological insights from 108 schizophrenia-associated genetic loci. *Nature* 511, 421–427.
- Schneider, C.A., Rasband, W.S., and Eliceiri, K.W. (2012). NIH Image to ImageJ: 25 years of image analysis. *Nat. Methods* 9, 671–675.
- Schork, A.J., Thompson, W.K., Pham, P., Torkamani, A., Roddey, J.C., Sullivan, P.F., Kelsoe, J.R., O'Donovan, M.C., Furberg, H., Schork, N.J., et al.; Tobacco and Genetics Consortium; Bipolar Disorder Psychiatric Genomics Consortium; Schizophrenia Psychiatric Genomics Consortium (2013). All SNPs are not created equal: genome-wide association studies reveal a consistent pattern of enrichment among functionally annotated SNPs. *PLoS Genet.* 9, e1003449.
- Shulha, H.P., Cheung, I., Whittle, C., Wang, J., Virgil, D., Lin, C.L., Guo, Y., Les-sard, A., Akbarian, S., and Weng, Z. (2012). Epigenetic signatures of autism: trimethylated H3K4 landscapes in prefrontal neurons. *Arch. Gen. Psychiatry* 69, 314–324.
- Shulha, H.P., Cheung, I., Guo, Y., Akbarian, S., and Weng, Z. (2013). Coordinated cell type-specific epigenetic remodeling in prefrontal cortex begins before birth and continues into early adulthood. *PLoS Genet.* 9, e1003433.
- Sklar, P., Smoller, J.W., Fan, J., Ferreira, M.A., Perlis, R.H., Chambert, K., Nimgaonkar, V.L., McQueen, M.B., Faraone, S.V., Kirby, A., et al. (2008). Whole-genome association study of bipolar disorder. *Mol. Psychiatry* 13, 558–569.
- Stahl, E.A., Raychaudhuri, S., Remmers, E.F., Xie, G., Eyre, S., Thomson, B.P., Li, Y., Kurreeman, F.A., Zhernakova, A., Hinks, A., et al.; BIRAC Consortium; YEAR Consortium (2010). Genome-wide association study meta-analysis identifies seven new rheumatoid arthritis risk loci. *Nat. Genet.* 42, 508–514.
- Tesli, M., Skatun, K.C., Ousdal, O.T., Brown, A.A., Thoresen, C., Agartz, I., Melle, I., Djurovic, S., Jensen, J., and Andreassen, O.A. (2013). CACNA1C risk variant and amygdala activity in bipolar disorder, schizophrenia and healthy controls. *PLoS ONE* 8, e56970.

- Trynka, G., Sandor, C., Han, B., Xu, H., Stranger, B.E., Liu, X.S., and Raychaudhuri, S. (2013). Chromatin marks identify critical cell types for fine mapping complex trait variants. *Nat. Genet.* 45, 124–130.
- Visel, A., Taher, L., Girgis, H., May, D., Golonzhka, O., Hoch, R.V., McKinsey, G.L., Pattabiraman, K., Silberberg, S.N., Blow, M.J., et al. (2013). A high-resolution enhancer atlas of the developing telencephalon. *Cell* 152, 895–908.
- Wenger, A.M., Clarke, S.L., Notwell, J.H., Chung, T., Tuteja, G., Guturu, H., Schaar, B.T., and Bejerano, G. (2013). The enhancer landscape during early neocortical development reveals patterns of dense regulation and co-option. *PLoS Genet.* 9, e1003728.
- Westra, H.J., Peters, M.J., Esko, T., Yaghootkar, H., Schurmann, C., Kettunen, J., Christiansen, M.W., Fairfax, B.P., Schramm, K., Powell, J.E., et al. (2013). Systematic identification of trans eQTLs as putative drivers of known disease associations. *Nat. Genet.* 45, 1238–1243.
- Xia, K., Shabalin, A.A., Huang, S., Madar, V., Zhou, Y.H., Wang, W., Zou, F., Sun, W., Sullivan, P.F., and Wright, F.A. (2012). seeQTL: a searchable database for human eQTLs. *Bioinformatics* 28, 451–452.
- Zhang, B.G., Bodea, L.G., Wang, Z., McElwee, J., Podtelezchnikov, A.A., Zhang, C., Xie, T., Tran, L., Dobrin, R., Fluder, E., et al. (2014). Tracing multi-system failure in Alzheimer disease to causal genes. *Cell*, X, in press.
- Zhong, H., Beaulaurier, J., Lum, P.Y., Molony, C., Yang, X., Macneil, D.J., Weingarh, D.T., Zhang, B., Greenawalt, D., Dobrin, R., et al. (2010). Liver and adipose expression associated SNPs are enriched for association to type 2 diabetes. *PLoS Genet.* 6, e1000932.
- Zhu, J., Adli, M., Zou, J.Y., Verstappen, G., Coyne, M., Zhang, X., Durham, T., Miri, M., Deshpande, V., De Jager, P.L., et al. (2013). Genome-wide chromatin state transitions associated with developmental and environmental cues. *Cell* 152, 642–654.